

Supplementary Materials for A Dynamic Network Model of mTOR Signaling Reveals TSC- Independent mTORC2 Regulation

Piero Dalle Pezze, Annika G. Sonntag, Antje Thien, Mirja T. Prentzell, Markus Gödel,
Sven Fischer, Elke Neumann-Haefelin, Tobias B. Huber, Ralf Baumeister,
Daryl P. Shanley,* Kathrin Thedieck*

*To whom correspondence should be addressed. E-mail: kathrin.thedieck@biologie.uni-freiburg.de (K.T.);
daryl.shanley@newcastle.ac.uk (D.P.S.)

Published 27 March 2012, *Sci. Signal.* **5**, ra25 (2012)
DOI: 10.1126/scisignal.2002469

This PDF file includes:

- Fig. S1. Extended graphical model of the mammalian TOR network.
- Fig. S2. A linear relationship between Western blot signals and protein concentrations.
- Fig. S3. Phases of the calibration process.
- Fig. S4. Details of a calibration phase.
- Fig. S5. Identifiability analysis for the general model.
- Fig. S6. Sensitivity analysis for the general model.
- Fig. S7. Comparison between the simulated and experimental time courses for hypotheses 1, 2, and 3 for readouts of the mTOR network.
- Fig. S8. Identifiability analysis for hypothesis 1: TSC1-TSC2-dependent hypothesis mTORC2 regulation.
- Fig. S9. Sensitivity analysis for hypothesis 1: TSC1-TSC2-dependent hypothesis mTORC2 regulation.
- Fig. S10. Identifiability analysis for hypothesis 2: NFL-mTORC2 regulation.
- Fig. S11. Sensitivity analysis for hypothesis 2: NFL-mTORC2 regulation.
- Fig. S12. Identifiability analysis for hypothesis 3: PI3K-independent mTORC2 regulation.
- Fig. S13. Sensitivity analysis for hypothesis 3: PI3K-independent mTORC2 regulation.
- Fig. S14. The influence of perturbations of TSC1-TSC2, mTORC1, and PI3K on the phosphorylation of Akt-T³⁰⁸ for the three hypotheses.
- Fig. S15. The influence of perturbations of TSC1-TSC2, mTORC1, and PI3K on the phosphorylation of p70-S6K-T³⁸⁹ for the three hypotheses.

Fig. S16. Simulation and perturbations for the new network structure based on hypothesis 4: PI3K-dependent, NFL-independent regulation of mTORC2.

Fig. S17. Identifiability analysis for hypothesis 4: PI3K-dependent, NFL-independent regulation of mTORC2.

Fig. S18. Sensitivity analysis for hypothesis 4: PI3K-dependent, NFL-independent regulation of mTORC2.

Table S1. Ordinary differential equations of the general model and the models representing hypotheses, 1, 2, and 3 for mTORC2 activation.

Table S2. Parameter values of the general model.

Table S3. Parameter values of hypotheses 1, 2, and 3.

Table S4. Summary of model goodness of fit.

Legends for Models S1 to S6.

Other Supplementary Material for this manuscript includes the following:

(available at www.sciencesignaling.org/cgi/content/full/5/217/ra25/DC1)

Models S1 to S6 (.xml format).

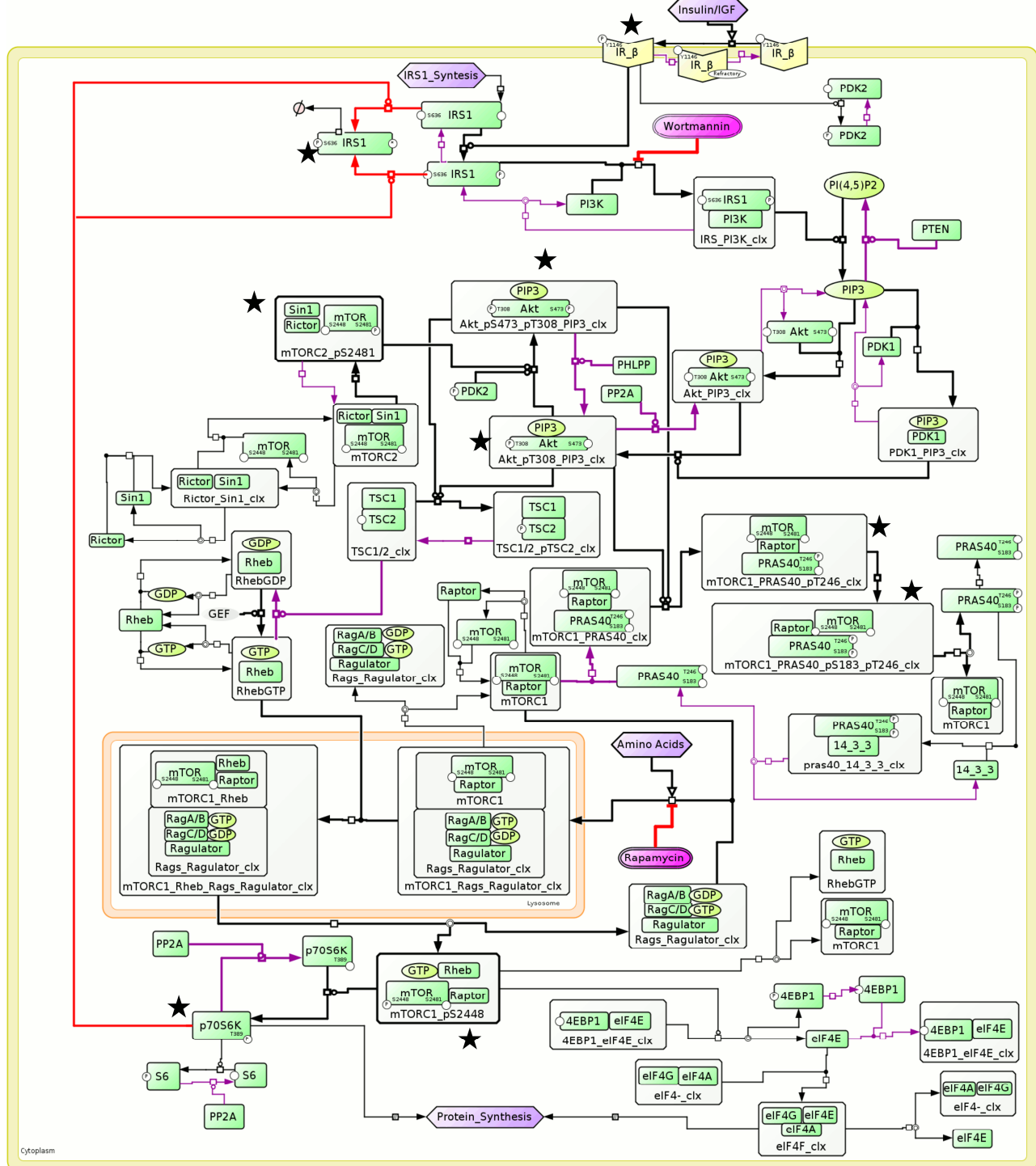


Fig. S1. Extended graphical model of the mammalian TOR network. A static network model of TOR signaling stimulated by amino acids plus insulin (aa/insulin) is shown in SBGN notation. This model integrates the current knowledge and guided our decision on appropriate targets for measurement. The selected targets are marked with an asterisk.

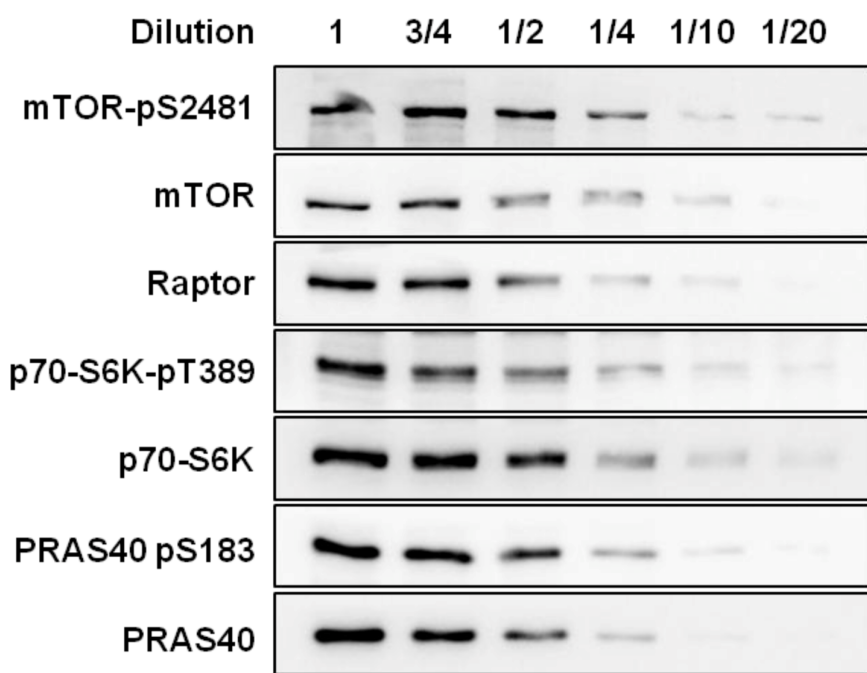


Fig. S2. A linear relationship between Western blot signals and protein concentrations. HeLa cells were lysed and cell lysates were diluted as indicated and analyzed by Western blotting. The linearity of signal to protein amount ratio was confirmed for selected antibodies used in this study.

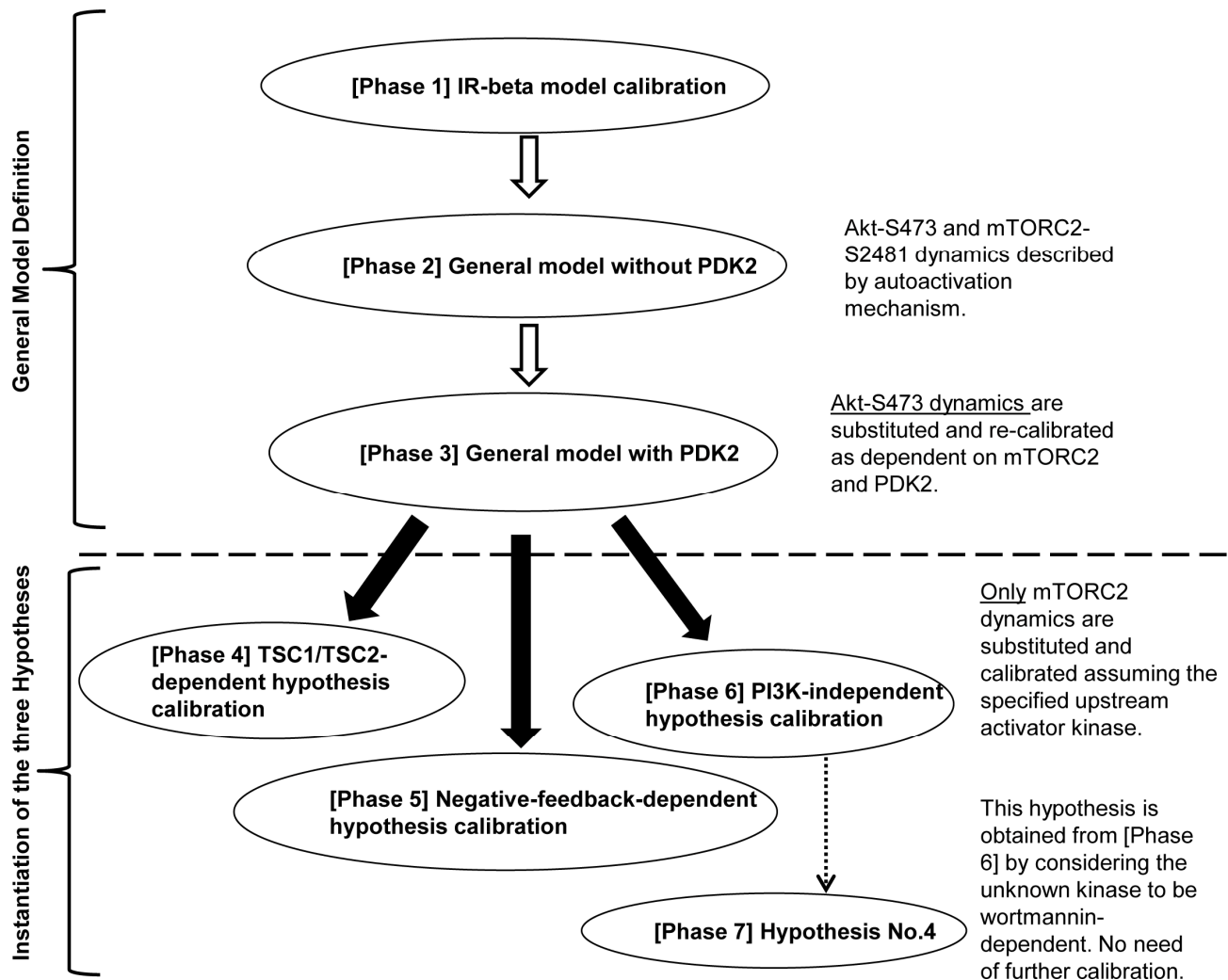


Fig. S3. Phases of the calibration process. The approach for defining our model was hierarchical and structured in two main parts. Part 1 (Phases 1-3) was the development of a general model without regulation of mTORC2 and part 2 was the introduction of specific hypotheses for regulation of mTORC2. In Phase 1, the kinetic rate constants of the insulin receptor were calibrated independently because the insulin receptor module was not regulated by the rest of the network. In Phase 2, the kinetic rate constants for the model representing the entire network without PDK2 were calibrated, assuming that the phosphorylation dynamics of mTOR-S2481 and Akt-S473 dynamics were regulated by autoactivation. In Phase 3, PDK2 was added to the network and the autoregulation mechanism controlling phosphorylation of Akt-S473 was replaced with the regulation by both mTORC2 and PDK2. Part 2 (Phases 4-6) of the calibration process concerned the introduction of the three hypotheses (Hypothesis 1,2, and 3) for mTORC2 activation from the general model defined in part 1 (Phase 3). The development and calibration of these hypotheses only required substitution of the mTORC2 dynamics of the general model with the specific regulation of the corresponding hypothesis and then recalibration of these new kinetic parameters. In Phase 7, Hypothesis 4 was obtained from the PI3K-independent model by transforming the unknown kinase into one dependent on Wortmannin, which did not involve further calibration.

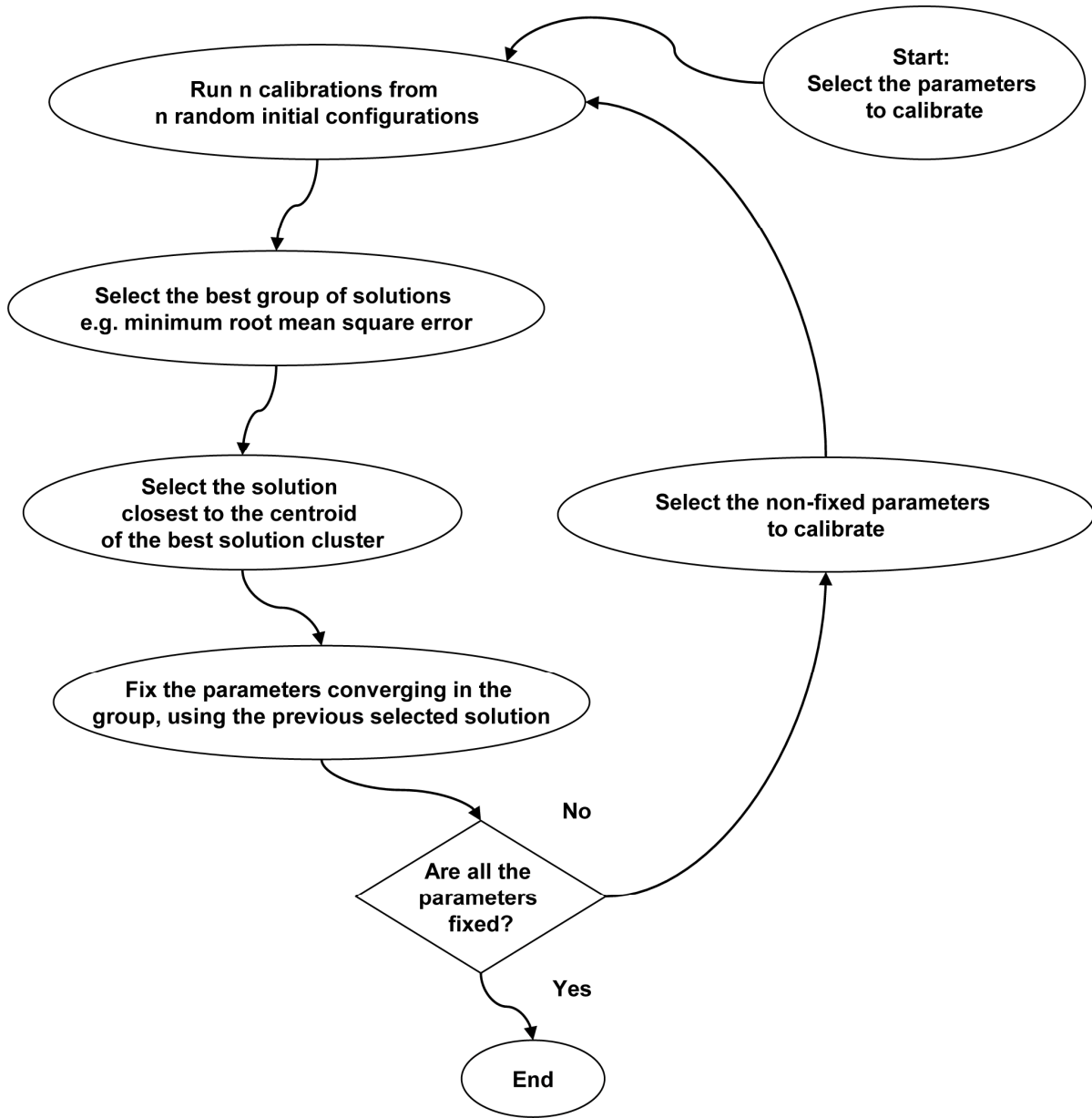


Fig. S4. Details of a calibration phase. The flow chart shows the details of the parameter calibration procedure. The procedure began with the selection of the set of parameters to estimate. After completing the calibrations, the procedure selected the subset of the solutions that obtained the minimum root mean square error (best solutions). The closest solution to the centroid of the best solution cluster was selected and the values common to all the solutions were fixed. All the parameters that were not fixed were selected for the next step of calibration. The procedure terminated when there were no further parameters to calibrate. In our model calibration, all the parameters were identified in only one iteration step.

General Model (Phase 3)
Parameter Correlation Matrix (absolute values)

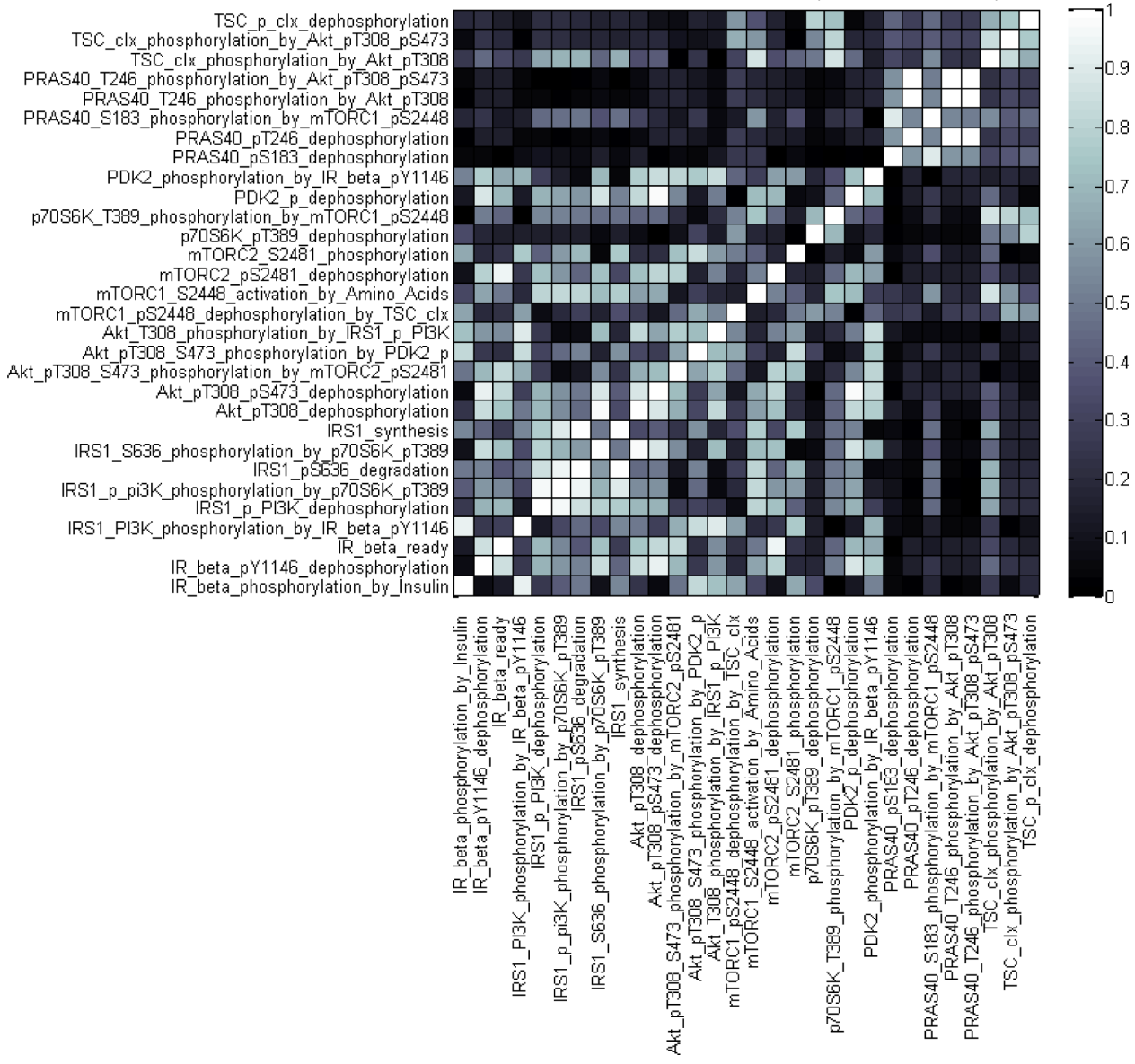


Fig. S5. Identifiability analysis for the general model. Parameter identifiability is based on sensitivity analysis and parameter correlation as computed by SBPD Matlab Toolbox. The symmetric matrix shows the parameter correlation in absolute values. High parameter correlations suggest potential issues in identifying the corresponding parameters independently (the elements on the diagonal obviously have correlation equal to 1). Conversely, low parameter correlations indicate that the corresponding parameters can be identified independently. Our experimental data were used in computing the reported identifiability analysis.

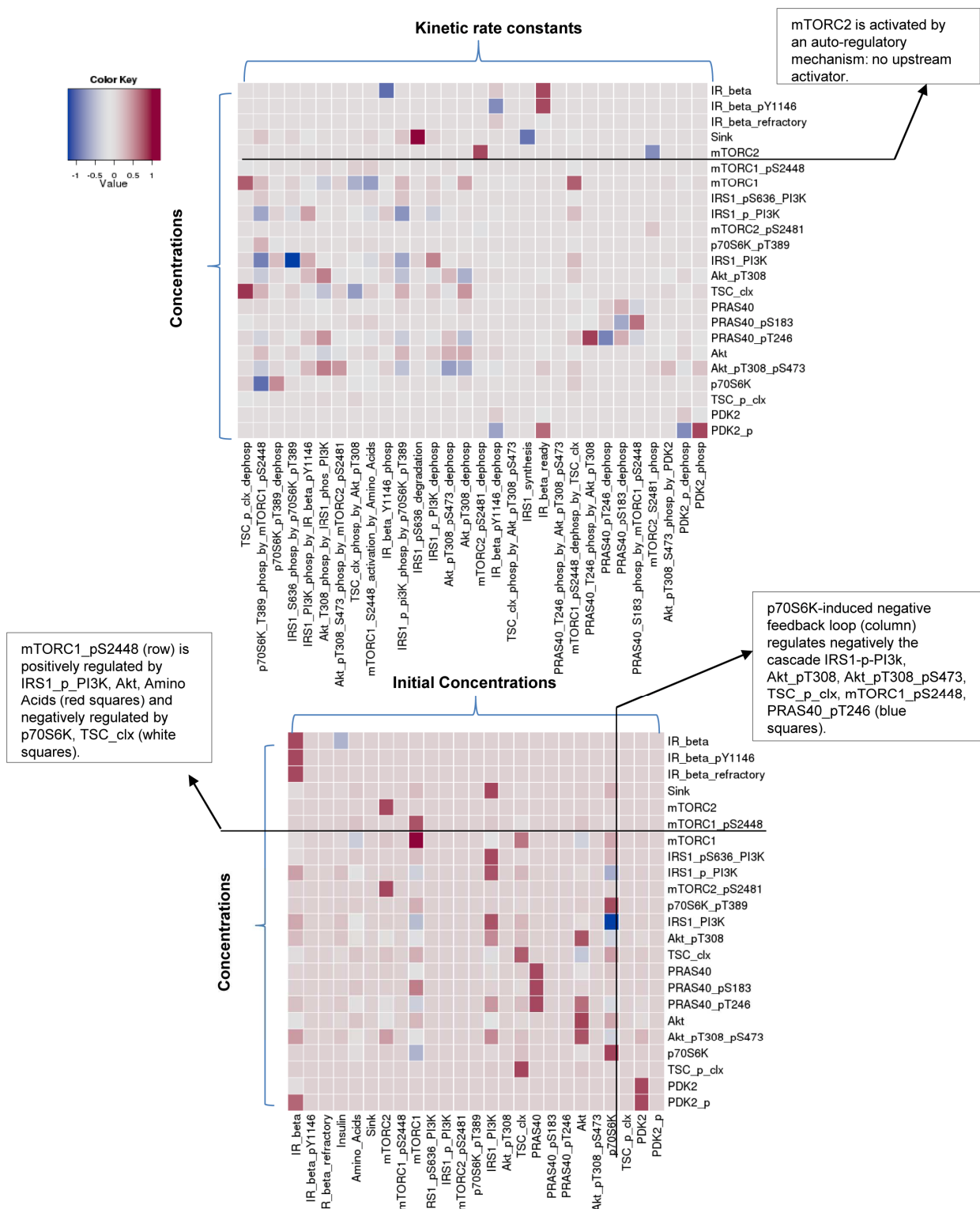
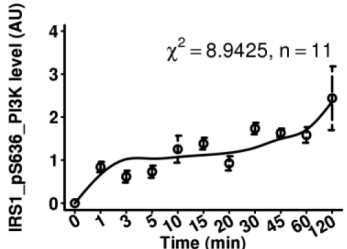
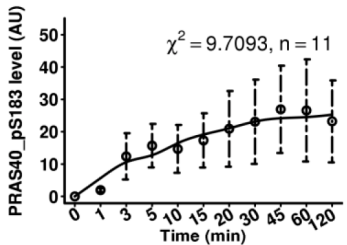
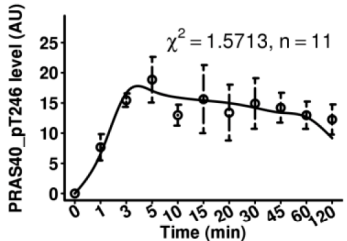
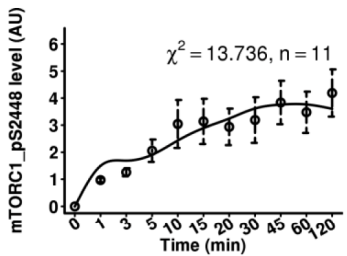
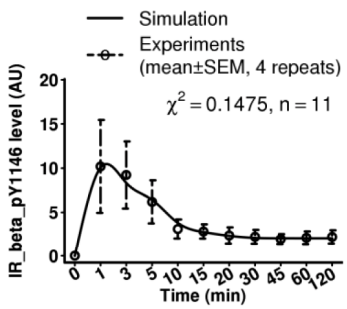
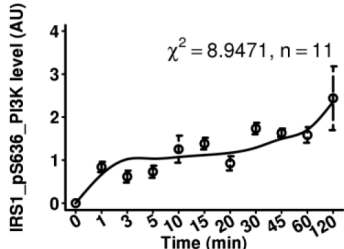
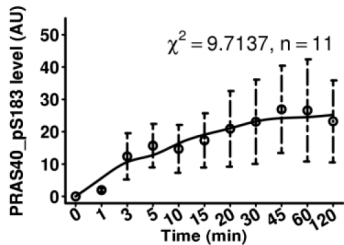
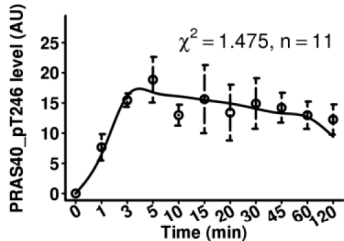
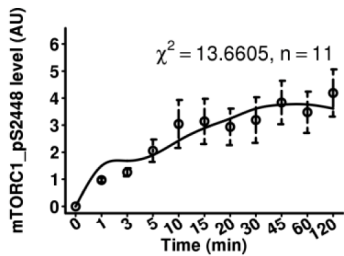
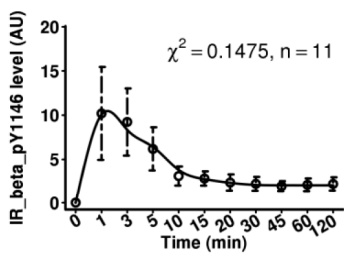


Fig. S6. Sensitivity analysis for the general model. The top plot illustrates the sensitivity analysis of the model by row, in response to the perturbations of the kinetic rates constants shown in columns. The bottom plot shows the model sensitivity analysis of the initial concentrations of the modelled species by row with perturbations shown in columns. Values were normalized in the range [-1, 1]. Positive values (red squares) represent positive regulation; negative ones (white-blue squares) represent inhibition.

Hypothesis 1: TSC1/TSC2-dependent



Hypothesis 2: NFL-dependent



Hypothesis 3: PI3K-independent

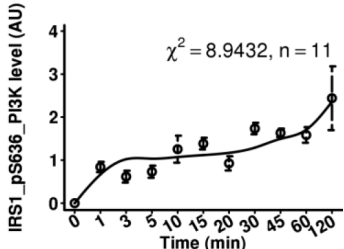
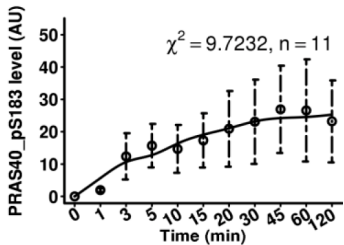
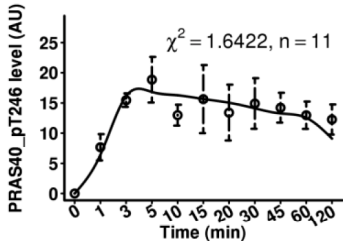
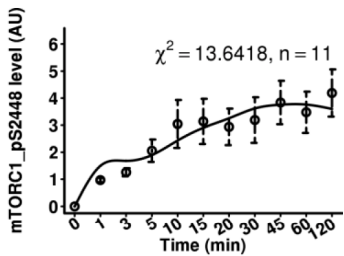
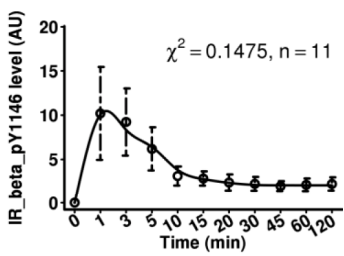
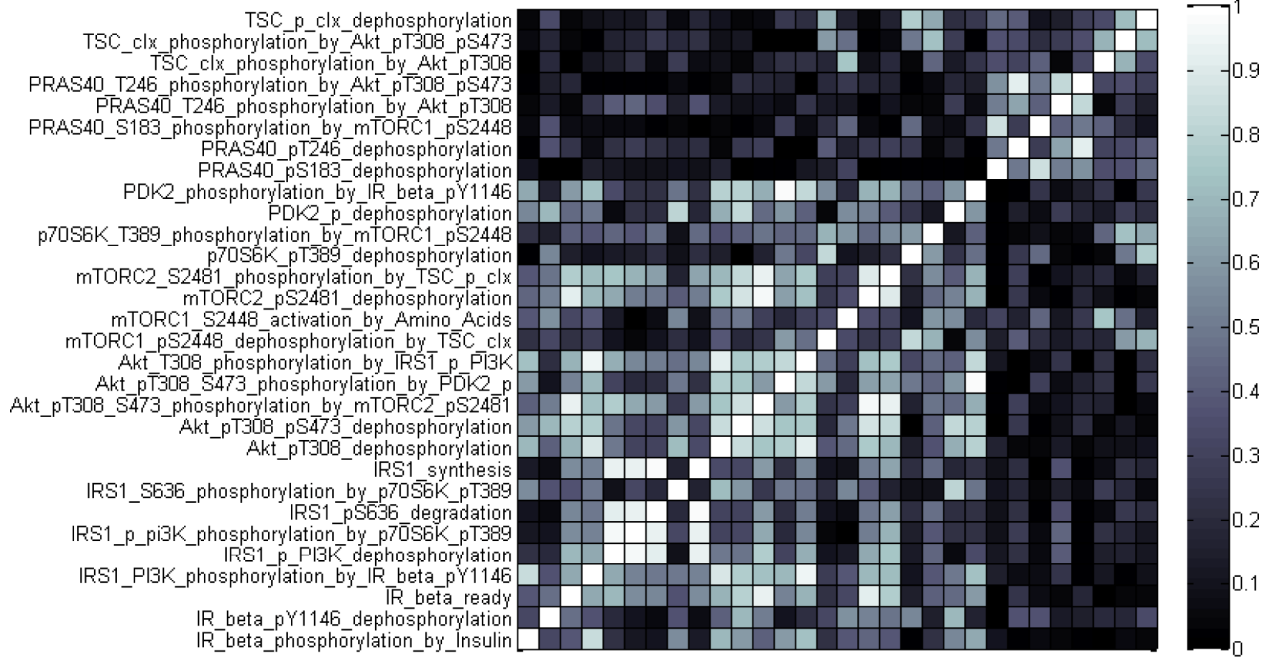


Fig. S7. Comparison between the simulated and experimental time courses for hypothesis 1, 2, and 3 for readouts of the mTOR network. The three hypotheses were consistent with each other for all the readouts indicating that introducing each hypothesis into the general model did not perturb the network. NFL = Negative Feedback Loop.

TSC1/TSC2-dependent Hypothesis (Phase 4)
Parameter Correlation Matrix (absolute values)



IR_beta_pY1146_dephosphorylation_by_Insulin
 IR_beta_pY1146_dephosphorylation_by_IR_beta_ready
 IRS1_Pi3K_phosphorylation_by_IR_beta_pY1146
 IRS1_p_Pi3K_phosphorylation_by_IR_beta_pY1146
 IRS1_pS636_degradation
 IRS1_p_Pi3K_dephosphorylation
 IRS1_Pi3K_phosphorylation_by_IR_beta_pY1146
 IR_beta_ready
 IR_beta_pY1146_dephosphorylation
 IR_beta_phosphorylation_by_Insulin
 Akt_pT308_S473_dephosphorylation_by_mTORC2_pS2481
 Akt_pT308_S473_phosphorylation_by_PDK2_p
 Akt_T308_phosphorylation_by_IRS1_p_Pi3K
 mTORC1_pS2448_dephosphorylation_by_TSC_clx
 mTORC1_S2448_activation_by_Amino_Acids
 mTORC2_pS2481_dephosphorylation_by_TSC_p_clx
 mTORC2_S2481_phosphorylation_by_TSC_p_clx
 p70S6K_pT389_dephosphorylation
 p70S6K_T389_phosphorylation_by_mTORC1_pS2448
 PDK2_p_dephosphorylation_by_IR_beta_pY1146
 PRAS40_pS183_dephosphorylation
 PRAS40_pT246_dephosphorylation_by_mTORC1_pS2448
 PRAS40_S183_phosphorylation_by_Akt_pT308_pS473
 PRAS40_T246_phosphorylation_by_Akt_pT308_pS473
 TSC_clx_phosphorylation_by_Akt_pT308_pS473
 TSC_p_clx_dephosphorylation

Fig. S8. Identifiability analysis for hypothesis 1: TSC1-TSC2-dependent hypothesis mTORC2 regulation. Parameter correlation matrix for TSC1/TSC2-dependent hypothesis is shown. See fig. S5 for details.

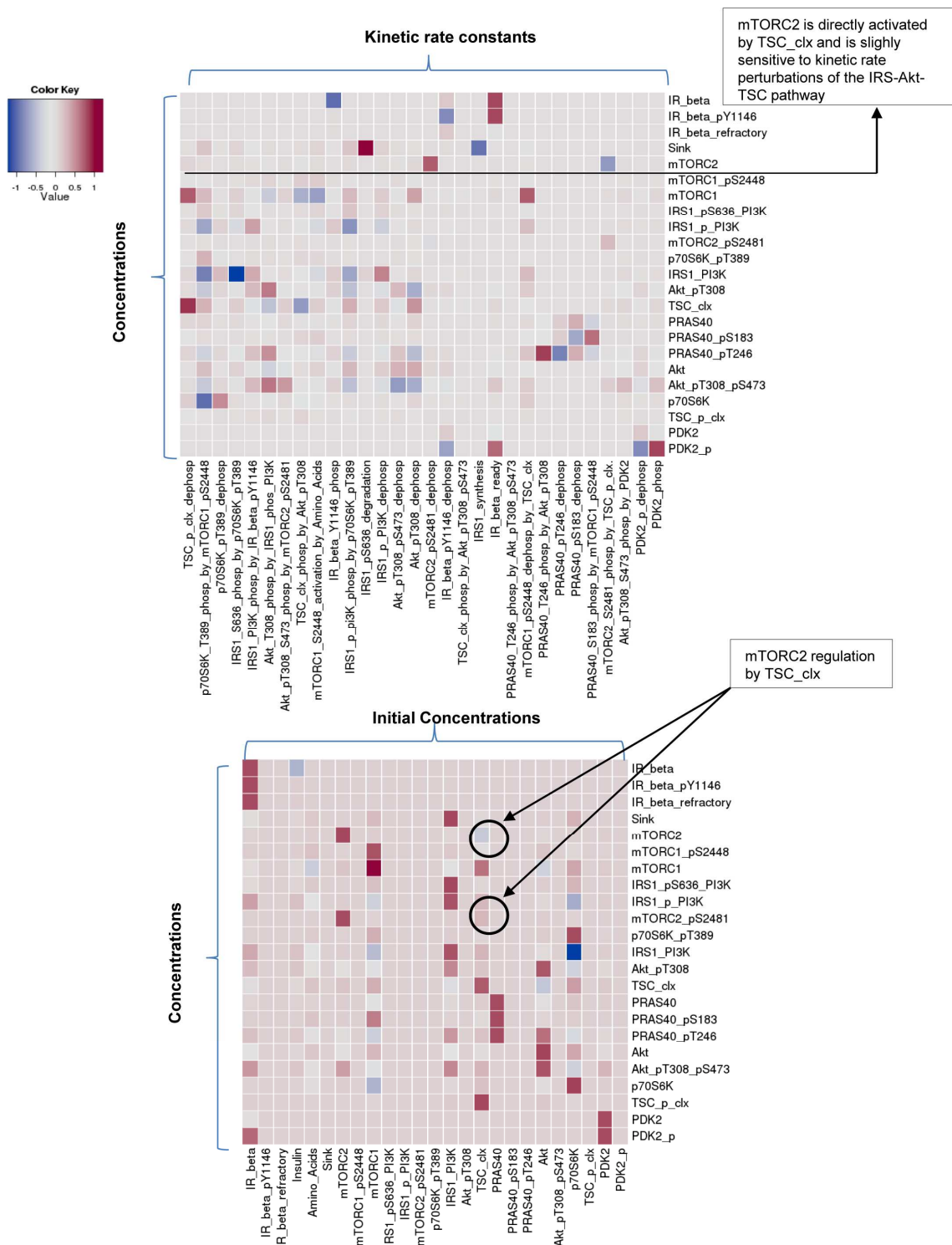


Fig. S9. Sensitivity analysis for hypothesis 1: TSC1-TSC2-dependent hypothesis mTORC2 regulation. The sensitivity analyses of the three hypotheses (see fig. S11 and S13) showed a similar sensitivity analysis excluding the sensitivity for the parameters characterizing each specific hypothesis. This provided evidence that the proposed general model (common to the three hypotheses) behaved in a consistent manner following introduction of the three hypothetical models and, therefore, the three models were comparable. See fig. S6 for details of the top and bottom plots.

NFL-dependent Hypothesis (Phase 5)
Parameter Correlation Matrix (absolute values)

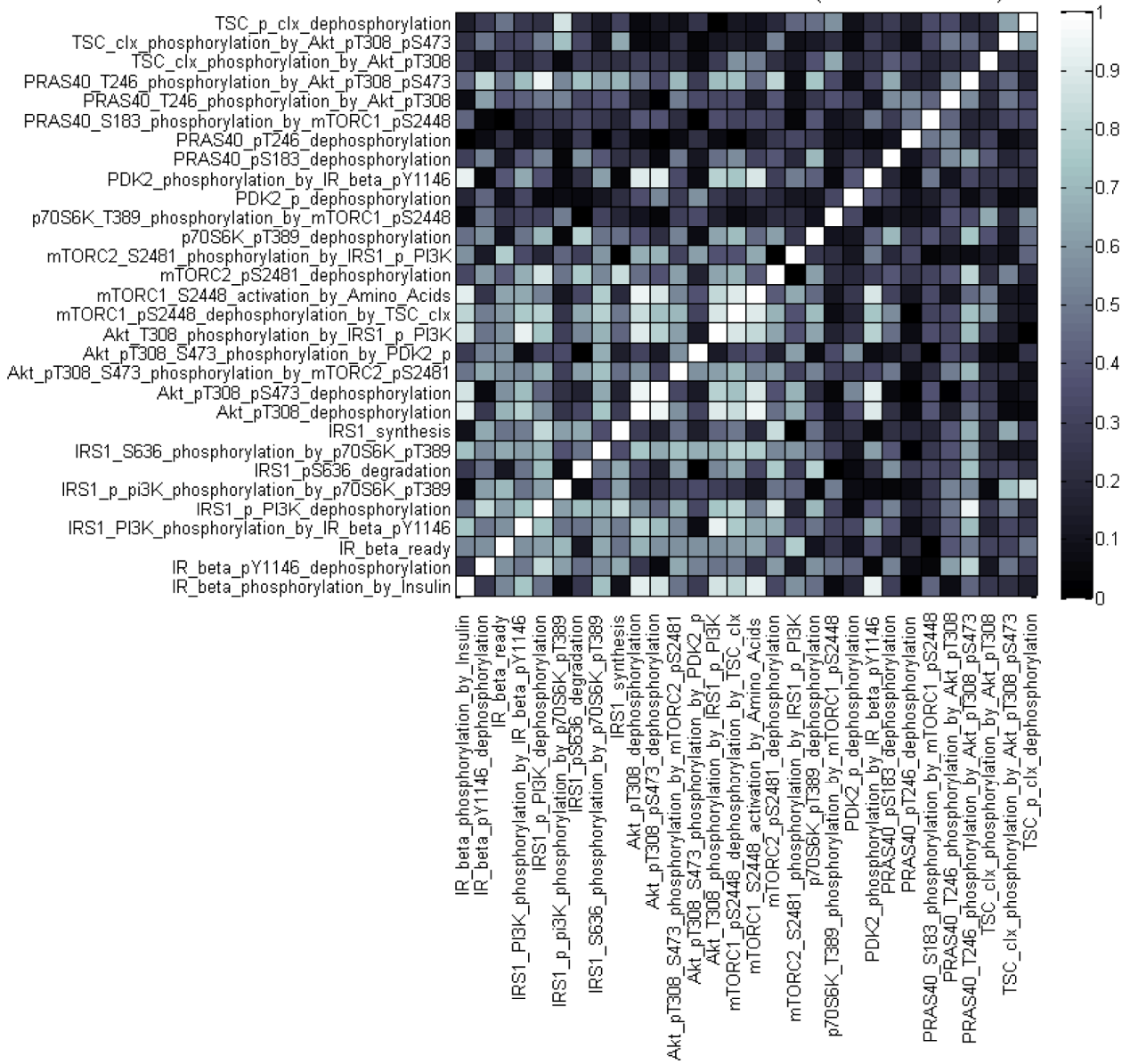


Fig. S10. Identifiability analysis for hypothesis 2: NFL-mTORC2 regulation.
Parameter correlation matrix for NFL-dependent hypothesis is shown. See fig. S5 for details.

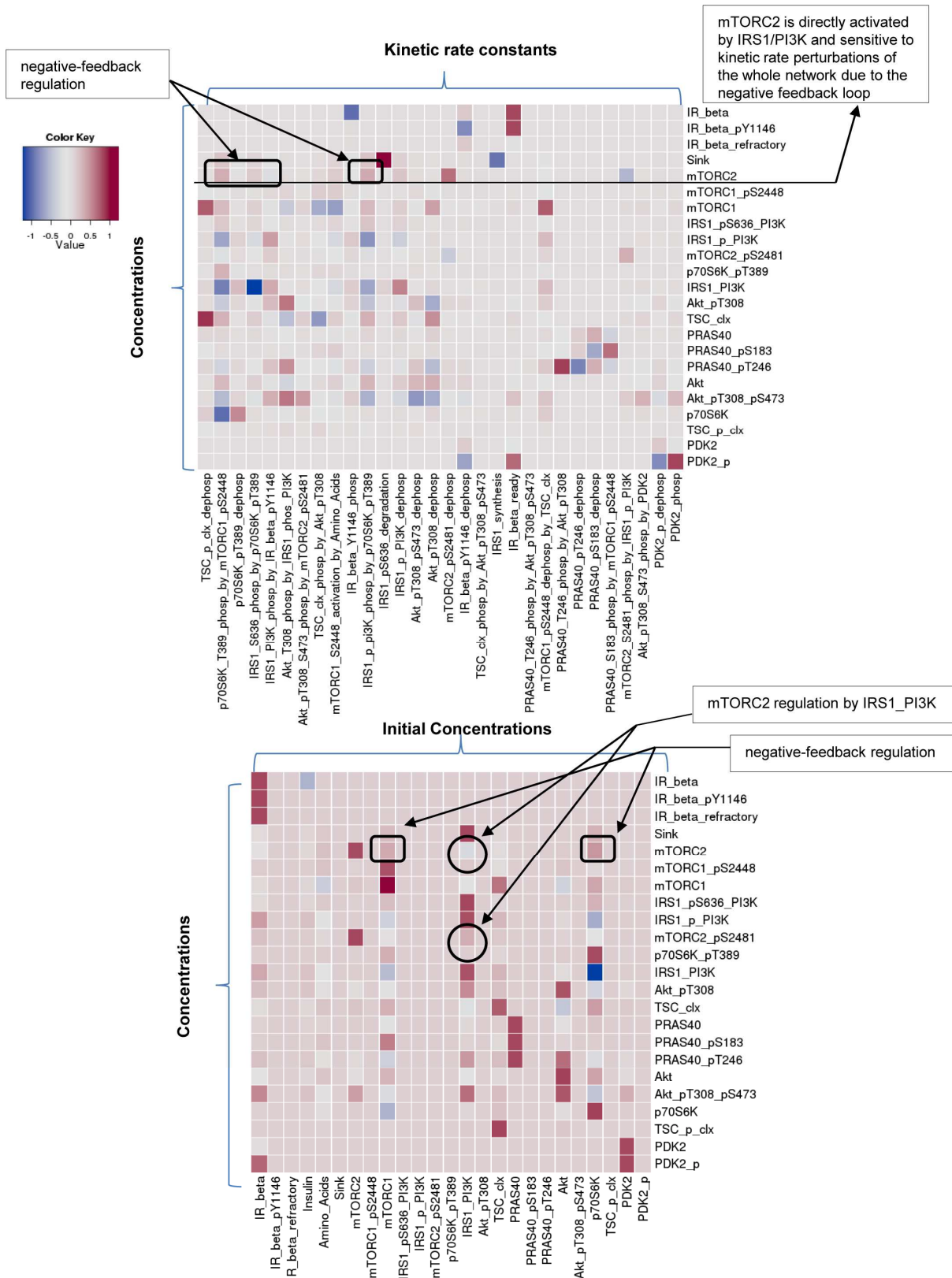


Fig. S11. Sensitivity analysis for hypothesis 2: NFL-mTORC2 regulation. Sensitivity analysis for the initial concentrations and the kinetic rates parameters for the NFL-dependent hypothesis is shown. See fig. S6 for details of the top and bottom plots.

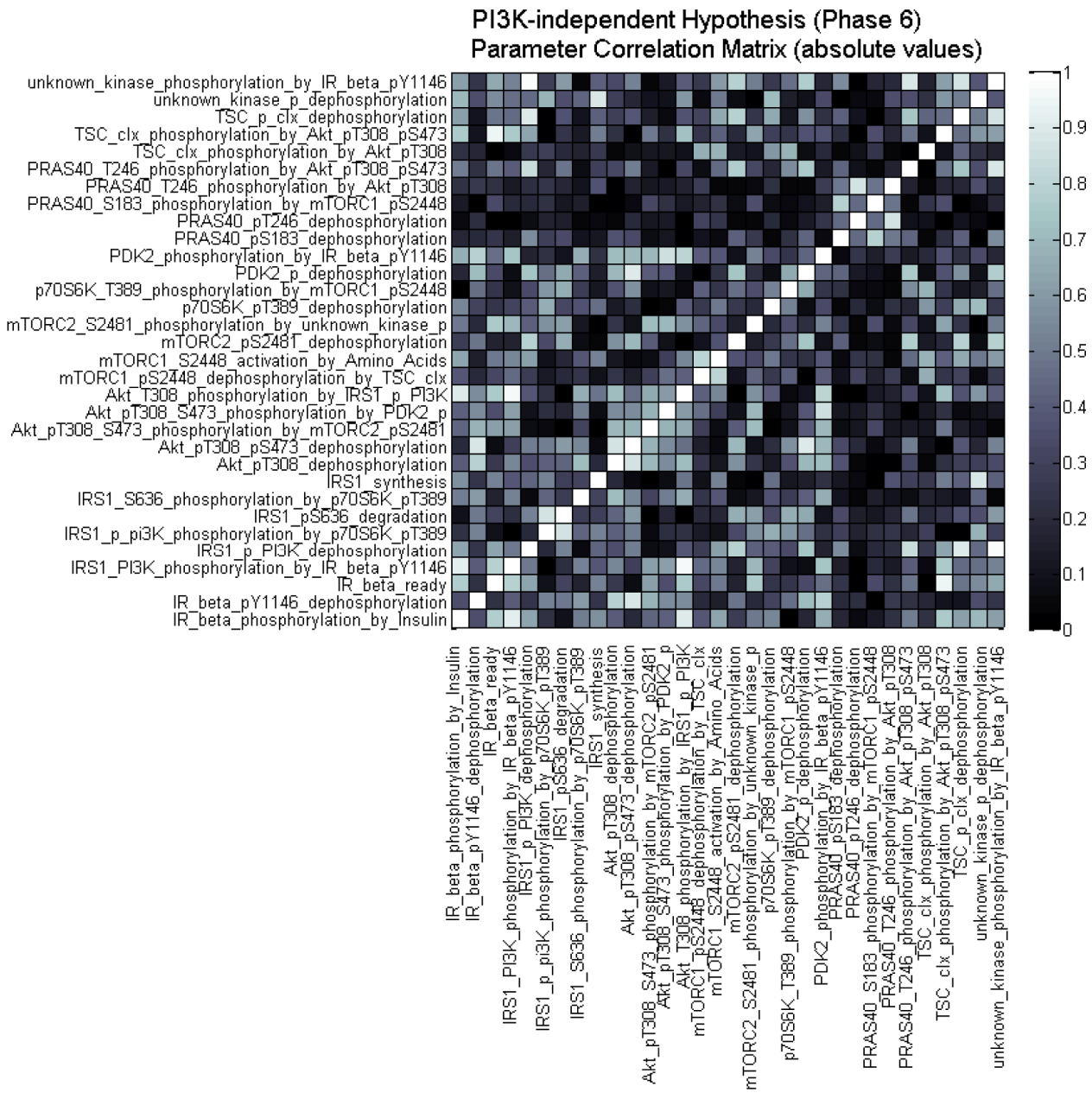


Fig. S12. Identifiability analysis for hypothesis 3: PI3K-independent mTORC2 regulation. Parameter correlation matrix for PI3K-independent hypothesis is shown. See fig. S5 for details.

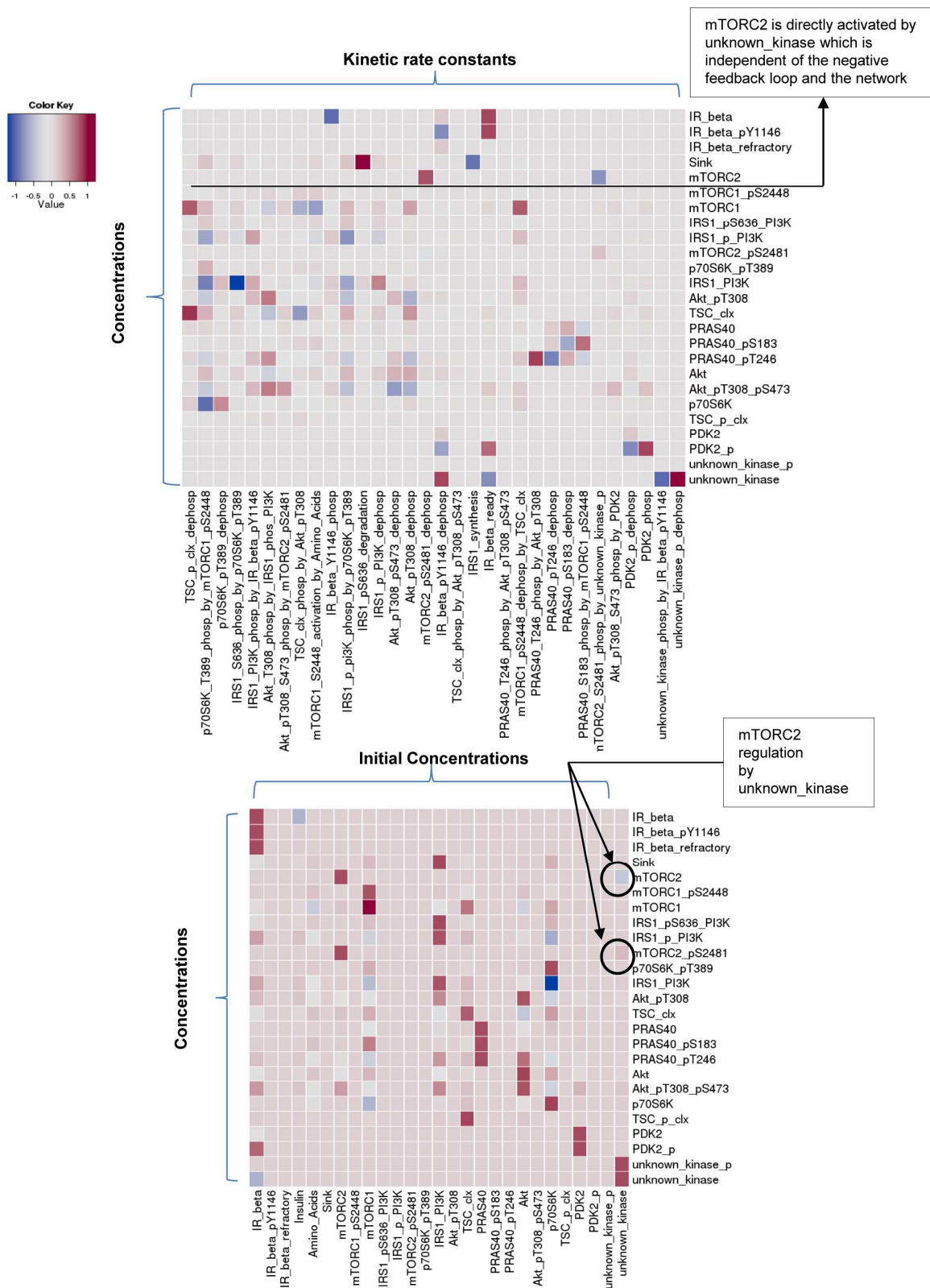


Fig. S13. Sensitivity analysis for hypothesis 3: PI3K-independent mTORC2 regulation. Sensitivity analysis for the initial concentrations and the kinetic rates parameters for the PI3K-independent hypothesis is shown. See fig. S6 for details of the top and bottom plots.

Akt-T308 readout

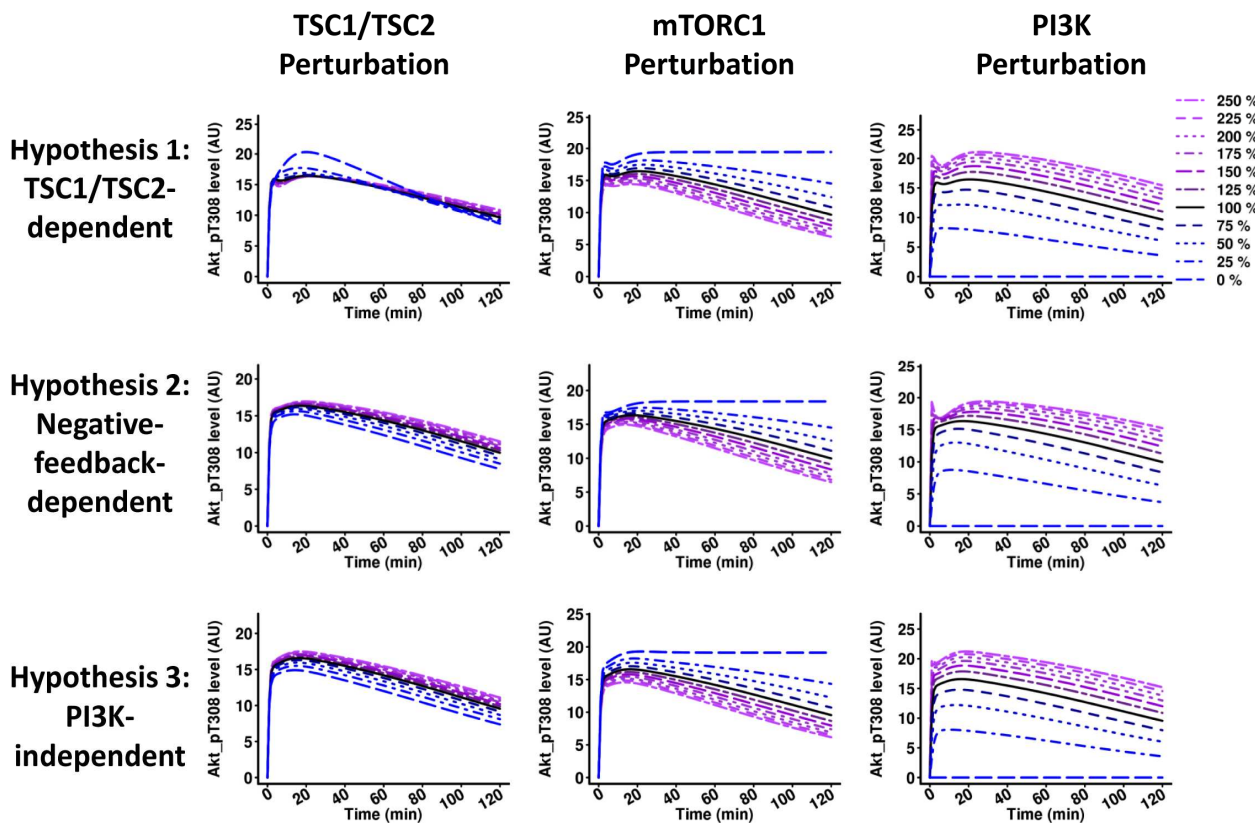


Fig. S14. The influence of perturbations of TSC1-TSC2, mTORC1, and PI3K on the phosphorylation of Akt-T³⁰⁸ for the three hypotheses. The three hypotheses did not show any difference in the dynamics of Akt-T308 phosphorylation when varying the amounts of PI3K and mTORC1. A small difference was observed for TSC1/TSC2 perturbation where the TSC1/TSC2-dependent hypothesis showed a slight increase in Akt-T308 phosphorylation when TSC1/TSC2 activity was reduced. In the TSC1/TSC2-dependent hypothesis, the mTORC2 activity is reduced when the amount of TSC1/TSC2 is reduced.

p70-S6K-T389 readout

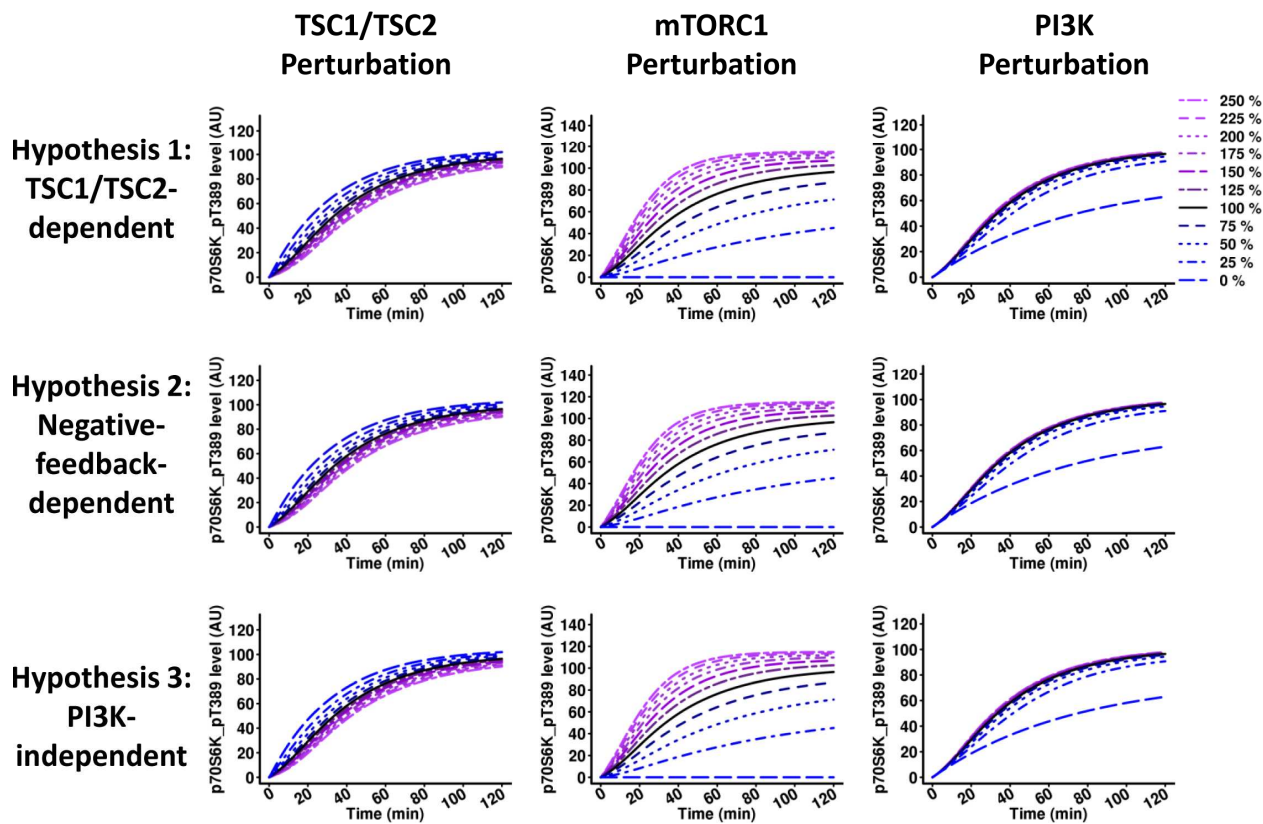
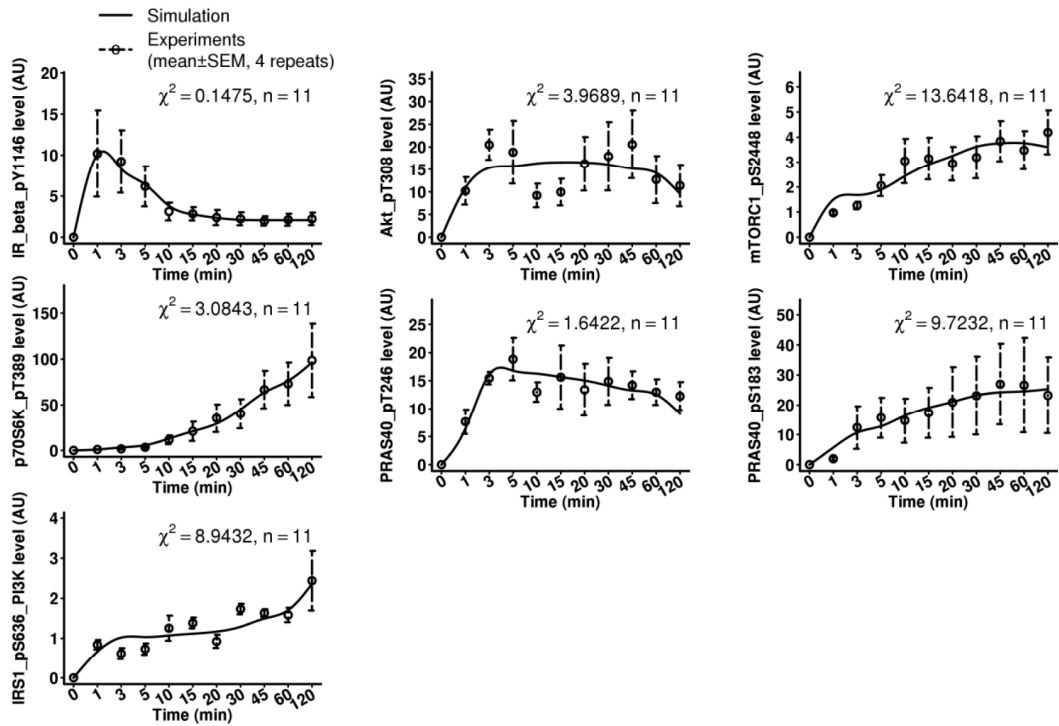


Fig. S15. The influence of perturbations of TSC1-TSC2, mTORC1, and PI3K on the phosphorylation of p70-S6K-T³⁸⁹ for the three hypotheses. The effect of each perturbation on the networks representing each hypothesis for the phosphorylation of p70-S6K-T389, which is a readout for mTORC1 activity, is shown.

**A) Simulated time courses versus experimental data for hypothesis No.4
(negative-feedback-independent, PI3K-dependent)**



B) Influence of perturbations of TSC1/TSC2, mTORC1 and PI3K on the Akt-T308 and p70-S6K-T389 readouts for hypothesis No.4.

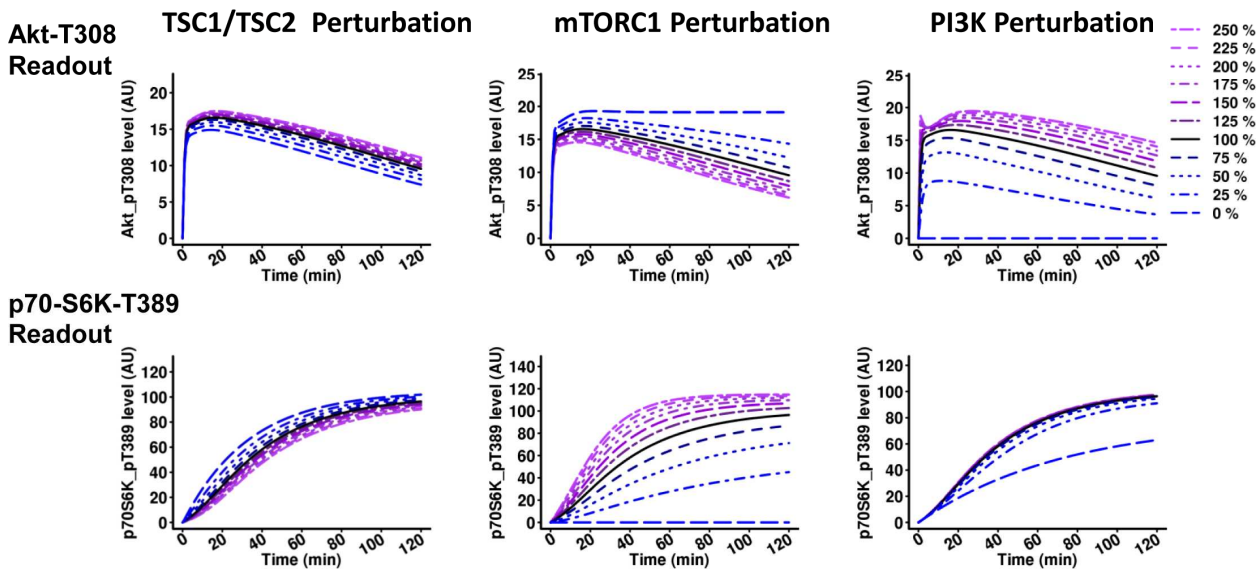


Fig. S16. Simulation and perturbations for the new network structure based on hypothesis 4: PI3K-dependent, NFL-independent regulation of mTORC2. (A)
Comparison between the simulated and experimental time courses for Hypothesis 4 shows that the simulated time courses match the experimental readouts. **(B)** The influence of perturbations of TSC1/TSC2, mTORC1, or PI3K on the dynamics of phosphorylation of Akt-T308 and p70-S6K-T389 for Hypothesis 4.

Hypothesis No.4 (Phase 7)
Parameter Correlation Matrix (absolute values)

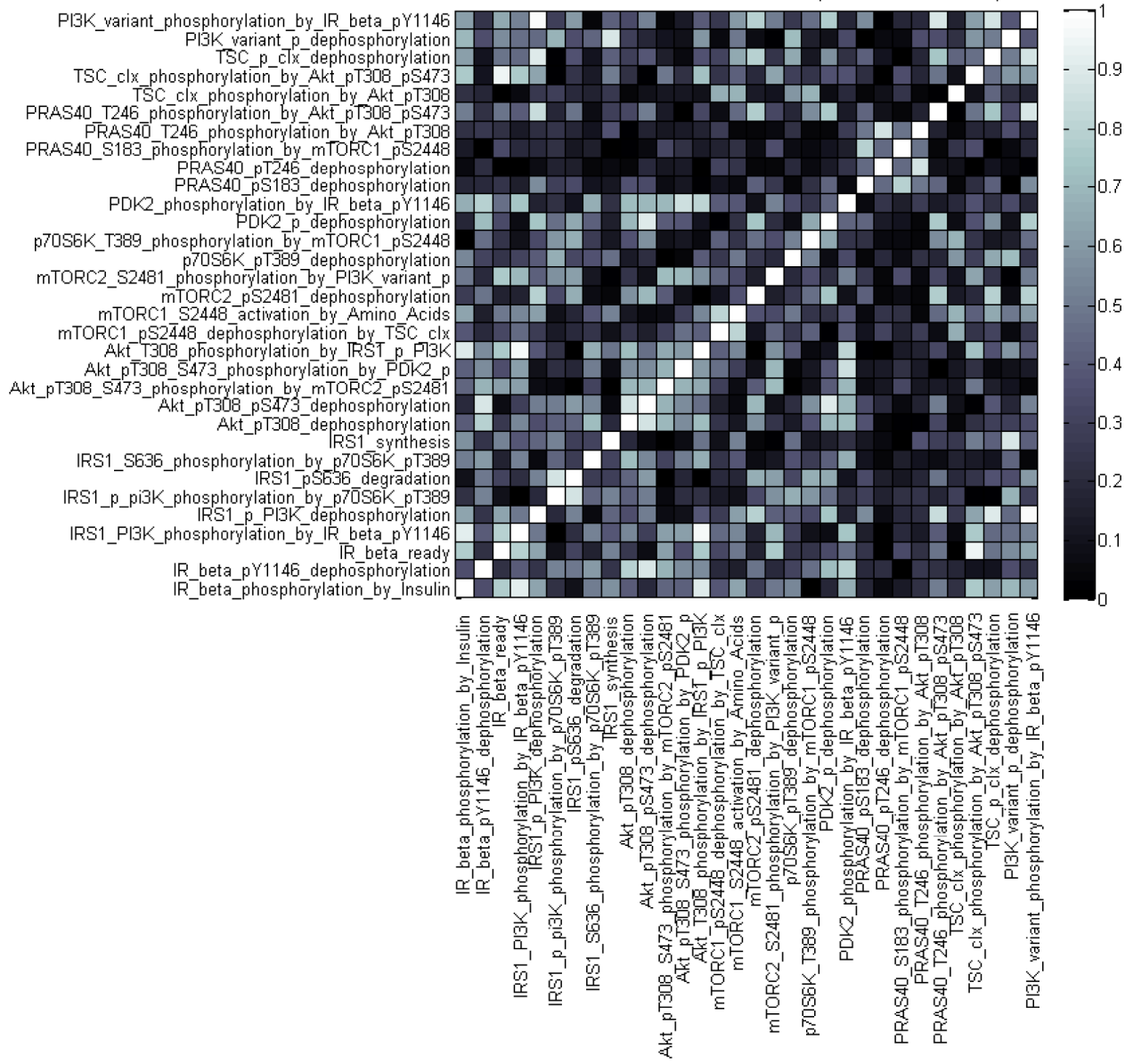


Fig. S17. Identifiability analysis for hypothesis 4: PI3K-dependent, NFL-independent regulation of mTORC2. Parameter correlation matrix for Hypothesis 4 is shown. See fig. S5 for details.

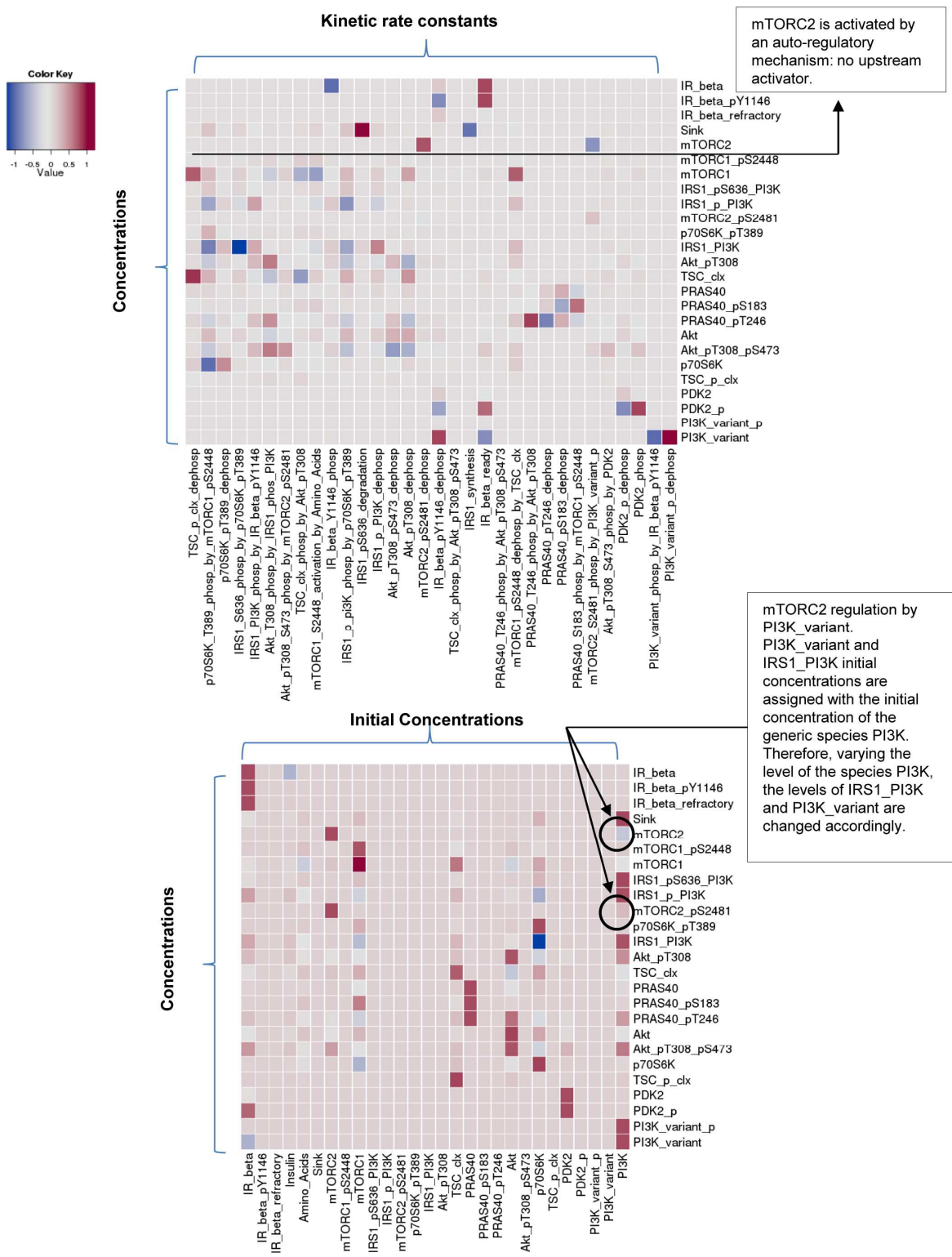


Fig. S18. Sensitivity analysis for hypothesis 4: PI3K-dependent, NFL-independent regulation of mTORC2. Sensitivity analysis for the initial concentrations and the kinetic rates parameters for Hypothesis 4 is shown. See fig. S6 for details of the top and bottom plots.

A) ODEs of the General Model

Parameters		Ordinary Differential Equations
Akt_pT308_dephosphorylation:	K ₁	Akt: $\dot{X}_1 = + K_1 \cdot X_2 - K_5 \cdot X_1 \cdot X_{10}$
Akt_pT308_ps473_dephosphorylation:	K ₂	Akt_pT308: $\dot{X}_2 = + K_2 \cdot X_3 - K_1 \cdot X_2 - K_4 \cdot X_2 \cdot X_{19} + K_5 \cdot X_1 \cdot X_{10} - K_3 \cdot X_2 \cdot X_{15}$
Akt_pT308_S473_phosphorylation_by_mTORC2_ps2481:	K ₃	Akt_pT308_ps473: $\dot{X}_3 = - K_2 \cdot X_3 + K_4 \cdot X_2 \cdot X_{19} + K_3 \cdot X_2 \cdot X_{15}$
Akt_pT308_S473_phosphorylation_by_PDK2:	K ₄	Amino_Acids: $\dot{X}_4 = \text{const}_{\text{ins}}$
Akt_T308_phosphorylation_by_IRS1_phos_PI3K:	K ₅	Insulin: $\dot{X}_5 = \text{const}_{\text{AA}}$
IR_beta_pY1146_dephosphorylation:	K ₆	IR_beta: $\dot{X}_6 = + K_7 \cdot X_8 - K_8 \cdot X_6 \cdot X_5$
IR_beta_ready:	K ₇	IR_beta_pY1146: $\dot{X}_7 = - K_6 \cdot X_7 + K_8 \cdot X_6 \cdot X_5$
IR_beta_Y1146_phosphorylation:	K ₈	IR_beta_refractory: $\dot{X}_8 = + K_6 \cdot X_7 - K_7 \cdot X_8$
IRS1_PI3K_phosphorylation_by_IR_beta_pY1146:	K ₉	IRS1_PI3K: $\dot{X}_9 = + K_{10} \cdot X_{10} + K_{14} \cdot X_{24} - K_{13} \cdot X_9 \cdot X_{17} - K_9 \cdot X_9 \cdot X_7$
IRS1_p_PI3K_dephosphorylation:	K ₁₀	
IRS1_p_pi3K_phosphorylation_by_p70S6K_pT389:	K ₁₁	
IRS1_pS636_degradation:	K ₁₂	
IRS1_S636_phosphorylation_by_p70S6K_pT389:	K ₁₃	IRS1_p_PI3K: $\dot{X}_{10} = - K_{11} \cdot X_{10} \cdot X_{17} - K_{10} \cdot X_{10} + K_{19} \cdot X_9 \cdot X_7$
IRS1_synthesis:	K ₁₄	
mTORC1_pS2448_dephosphorylation_by_TSC_clx:	K ₁₅	IRS1_pS636_PI3K: $\dot{X}_{11} = + K_{11} \cdot X_{10} \cdot X_{17} - K_{12} \cdot X_{11} + K_{13} \cdot X_9 \cdot X_{17}$
mTORC1_S2448_activation_by_Amino_Acids:	K ₁₆	mTORC1: $\dot{X}_{12} = + K_{15} \cdot X_{13} \cdot X_{24} - K_{16} \cdot X_{12} \cdot X_4$
mTORC2_ps2481_dephosphorylation:	K ₁₇	mTORC1_pS2448: $\dot{X}_{13} = - K_{15} \cdot X_{13} \cdot X_{24} + K_{16} \cdot X_{12} \cdot X_4$
mTORC2_S2481_phosphorylation:	K ₁₈	mTORC2: $\dot{X}_{14} = + K_{17} \cdot X_{15} - K_{18} \cdot X_{14}$
p70S6K_pT389_dephosphorylation:	K ₁₉	mTORC2_ps2481: $\dot{X}_{15} = - K_{17} \cdot X_{15} + K_{18} \cdot X_{14}$
p70S6K_T389_phosphorylation_by_mTORC1_pS2448:	K ₂₀	p70S6K: $\dot{X}_{16} = - K_{20} \cdot X_{16} \cdot X_{13} + K_{19} \cdot X_{17}$
PDK2_p_dephosphorylation:	K ₂₁	p70S6K_pT389: $\dot{X}_{17} = + K_{20} \cdot X_{16} \cdot X_{13} - K_{19} \cdot X_{17}$
PDK2_phosphorylation:	K ₂₂	PDK2: $\dot{X}_{18} = - K_{22} \cdot X_{18} \cdot X_7 + K_{21} \cdot X_{19}$
PRAS40_pS183_dephosphorylation:	K ₂₃	PDK2_p: $\dot{X}_{19} = + K_{22} \cdot X_{18} \cdot X_7 - K_{21} \cdot X_{19}$
PRAS40_pT246_dephosphorylation:	K ₂₄	PRAS40: $\dot{X}_{20} = - K_{27} \cdot X_{20} \cdot X_3 - K_{26} \cdot X_{20} \cdot X_2 + K_{24} \cdot X_{22} + K_{23} \cdot X_{21} - K_{25} \cdot X_{20} \cdot X_{13}$
PRAS40_S183_phosphorylation_by_mTORC1_ps2448:	K ₂₅	
PRAS40_T246_phosphorylation_by_Akt_pT308:	K ₂₆	PRAS40_pS183: $\dot{X}_{21} = - K_{23} \cdot X_{21} + K_{25} \cdot X_{20} \cdot X_{13}$
PRAS40_T246_phosphorylation_by_Akt_pT308_ps473:	K ₂₇	
TSC_clx_phosphorylation_by_Akt_pT308:	K ₂₈	PRAS40_pT246: $\dot{X}_{22} = + K_{27} \cdot X_{20} \cdot X_3 + K_{26} \cdot X_{20} \cdot X_2 - K_{24} \cdot X_{22}$
TSC_clx_phosphorylation_by_Akt_pT308_ps473:	K ₂₉	Sink: $\dot{X}_{23} = + K_{12} \cdot X_{11} - K_{14} \cdot X_{23}$
TSC_p_clx_dephosphorylation:	K ₃₀	TSC_clx: $\dot{X}_{24} = + K_{30} \cdot X_{25} - K_{29} \cdot X_{24} \cdot X_3 - K_{28} \cdot X_{24} \cdot X_2$
		TSC_p_clx: $\dot{X}_{25} = - K_{30} \cdot X_{25} + K_{29} \cdot X_{24} \cdot X_3 + K_{28} \cdot X_{24} \cdot X_2$

B) ODEs of the there Hypotheses

Parameters	
1 st Hypothesis	mTORC2_pS2481_dephosphorylation: K_{31} mTORC2_S2481_phosphorylation_by_TSC_p_clx: K_{32}
2 nd Hypothesis	mTORC2_pS2481_dephosphorylation: K_{33} mTORC2_S2481_phosphorylation_by_IRS1_phos_PI3K: K_{34}
3 rd Hypothesis	mTORC2_S2481_phosphorylation_by_unknown_kinase_p: K_{35} mTORC2_pS2481_dephosphorylation: K_{36} unknown_kinase_p_dephosphorylation: K_{37} unknown_kinase_phosphorylation_by_IR_beta_pY1146: K_{38}
Ordinary Differential Equations	
1 st Hypothesis	mTORC2: $\dot{X}_{26} = - K_{32} \cdot X_{26} \cdot X_{25} + K_{31} \cdot X_{27}$ mTORC2_pS2481: $\dot{X}_{27} = + K_{32} \cdot X_{26} \cdot X_{25} - K_{31} \cdot X_{27}$
2 nd Hypothesis	mTORC2: $\dot{X}_{28} = - K_{34} \cdot X_{28} \cdot X_{10} + K_{33} \cdot X_{29}$ mTORC2_pS2481: $\dot{X}_{29} = + K_{34} \cdot X_{28} \cdot X_{10} - K_{33} \cdot X_{29}$
3 rd Hypothesis	mTORC2: $\dot{X}_{30} = - K_{35} \cdot X_{30} \cdot X_{33} + K_{36} \cdot X_{31}$ mTORC2_pS2481: $\dot{X}_{31} = + K_{35} \cdot X_{30} \cdot X_{33} - K_{36} \cdot X_{31}$ unknown_kinase: $\dot{X}_{32} = - K_{38} \cdot X_{32} \cdot X_7 + K_{37} \cdot X_{33}$ unknown_kinase_p: $\dot{X}_{33} = + K_{38} \cdot X_{32} \cdot X_7 - K_{37} \cdot X_{33}$

These ODEs are substituted and instantiated for each hypothesis

Table S1. Ordinary differential equations of the general model and the models representing hypothesis 1, 2, and 3 for mTORC2 activation. List of kinetic rate constants and ordinary differential equations (ODEs) for the general model (A) and the Hypotheses 1, 2, and 3 (B). Each hypothesis is derived from the general model by replacing the mTORC2 ODEs, shown in the box, with those corresponding to the hypothesis.

Parameter Names	IR_beta model calibration [Phase 1 ; 3 parameters]	General model (no PDK2) [Phase 2 ; 24 parameters]	General model (+ PDK2) [Phase 3 ; 3 parameters]	Parameter Values
Kinetic Rate Constants (min⁻¹)				
Akt_pT308_dephosphorylation		4.0737591667 ± 0.0009002079	fixed	4.0739
Akt_pT308_pS473_dephosphorylation		2.113835 ± 0.0001043631	(replaced with the next reaction)	2.11397
Akt_pT308_pS473_dephosphorylation		9.9999975 ± 4.330127018e-06	(replaced with the next 2 reactions)	7.52842
Akt_pT308_S473_phosphorylation_(autoregulation)				9.99999
Akt_pT308_S473_phosphorylation_by_mTORC2_pS2481		4.5073187429 ± 0.0142519251		4.50769
Akt_pT308_S473_phosphorylation_by_PDK2		5.9038608857 ± 0.0168590452		5.90372
Akt_T308_phosphorylation_by_IRS1_phos_Pi3K	0.1493278 ± 2.92916370e-06	0.6994409167 ± 0.0001739753	fixed	0.699505
IR_beta_ready	0.030973095 ± 1.45639108e-06	fixed		0.149328
IR_beta_Y1146_phosphorylation	0.025376377 ± 5.51335650e-07	fixed		0.0309731
IRS1_Pi3K_phosphorylation_by_IR_beta_pY1146		0.1346880833 ± 1.9302237924e-05	fixed	0.0253763
IRS1_p_Pi3K_dephosphorylation		0.0032827042 ± 1.1067027479e-06	fixed	0.134664
IRS1_p_pi3K_phosphorylation_by_pT056K_pT389		0.0001 ± 2.7105054312e-20	fixed	0.00328283
IRS1_S636_degradation		0.0001000023 ± 2.1650635094e-09	fixed	0.000100001
IRS1_S636_phosphorylation_by_pT056K_pT389		0.999995 ± 5.0000000001e-07	fixed	1
IRS1_synthesis		0.0999933667 ± 5.4945933021e-06	fixed	0.9999968
mTORC1_pS2448_dephosphorylation_by_TSC_clx		0.9999950833 ± 4.0095372412e-06	fixed	0.999989
mTORC1_S2448_activation_by_Amino_Acids		0.05138455 ± 6.6251415079e-06	fixed	0.0513784
mTORC2_pS2481_dephosphorylation		0.0174131917 ± 1.795577127e-06	fixed	0.0174149
mTORC2_S2481_phosphorylation		0.0781611 ± 4.6502688094e-06	fixed	0.0781585
pT056K_pT389_dephosphorylation		0.0052853975 ± 2.2100683435e-06	fixed	0.00528455
pT056K_T389_phosphorylation_by_mTORC1_pS2448		0.0057393217 ± 5.0554975576e-07	fixed	0.00573896
PDK2_p_dephosphorylation			assumed	1
PDK2_phosphorylation			assumed	0.1
PRAS40_pS183_dephosphorylation		0.4034775533 ± 0.0001069866	fixed	0.403706
PRAS40_pT246_dephosphorylation		0.9999980833 ± 2.841898817e-06	fixed	0.999991
PRAS40_S183_phosphorylation_by_mTORC1_pS2448		0.073052733 ± 1.8625892968e-05	fixed	0.073093
PRAS40_T246_phosphorylation_by_Akt_pT308		0.0239171 ± 8.6986589004e-07	fixed	0.0239178
PRAS40_T246_phosphorylation_by_Akt_pT308_pS473		0.00010002083 ± 2.09993386e-09	fixed	0.000100001
TSC_clx_phosphorylation_by_Akt_pT308		0.0062716025 ± 1.4869326649e-06	fixed	0.00627315
TSC_clx_phosphorylation_by_Akt_pT308_pS473		0.00010009083 ± 9.79335091e-09	fixed	0.000100039
TSC_p_clx_dephosphorylation		0.0081260025 ± 3.274604619e-06	fixed	0.00812537
Protein Amounts (Arbitrary Unit – AU)				
Akt	determined	determined		144.13
Amino_Acids (input)	determined	determined		100
Insulin (input)				100
IR_beta				12.1175
IRS1_Pi3K		determined		2.965
mTORC1		determined		4.3225
mTORC2		determined		6.2175
pT056K		determined		127.0725
PDK2		determined	assumed = IR_beta	12.1175
PRAS40		assumed		73.2175
TSC_clx				10
Number of Estimated Solutions Sets:	1	2 (1 rejected as inconsistent with data)	1	

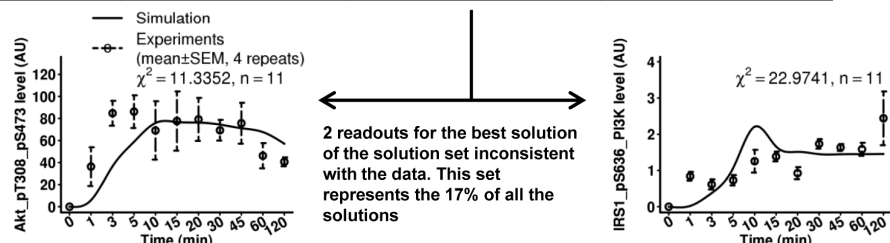


Table S2. Parameter values of the general model. The general model was fully parameterized by three steps. Phase 1, three kinetic rate constants of the insulin receptor (IR-beta) were determined. Phase 2, the general model without PDK2 was obtained by parameterizing 24 kinetic rate constants. In this phase, Akt-S473 activation is modelled as autoregulation, independent of mTORC2 and PDK2. Phase 3, PDK2 dynamics were added to the system and the three parameters regulating Akt-S473 phosphorylation were calibrated by substituting the previously introduced autoregulatory mechanism (parameters values shown in red) of Akt. For each phase, 350 independent calibrations, starting from random initial configurations of the parameters, were executed and the best solution set fitting the data was selected. Phase 1 and 3 converged to a single solution set. Phase 2 converged to two solutions sets of which one was discarded as inconsistent with the experimental data (shown for phosphorylated Akt-S473 and IRS1-S636 readouts). For each phase, the mean and standard deviation of the estimated parameters were computed from the selected solution set. The solution closest to the centroid of the selected solution cluster was chosen for fixing the parameter values.

Hypotheses	No. Estimated Solutions Sets:	Parameter Names	Hypotheses calibration	Parameter Values
Hypothesis No.1 (TSC1/TSC2-dependent) [Phase 4 ; 2 parameters]	1	Kinetic Rate Constants (min ⁻¹) mTORC2_pS2481_dephosphorylation mTORC2_S2481_phosphorylation_by_TSC_p_clx	0.2060607514 ± 0.0001069 0.0668916283 ± 3.03470106e-05	0.206059 0.0668912
Hypothesis No.2 (NFL-dependent) [Phase 5 ; 2 parameters]	1	mTORC2_pS2481_dephosphorylation mTORC2_S2481_phosphorylation_by_IRS1_phos_PI3K	0.0250001279 ± 1.5959455e-05 0.0561080757 ± 3.78781639e-06	0.025 0.0561081
Hypothesis No.3 (PI3K-independent) [Phase 6 ; 4 parameters]	1	mTORC2_S2481_phosphorylation_by_unknown_kinase mTORC2_pS2481_dephosphorylation unknown_kinase_p_dephosphorylation unknown_kinase_phosphorylation_by_IR_beta_pY1146	0.0318873566 ± 1.02655930e-05 0.0255700314 ± 1.631113942e-05 0.0002336665 ± 5.21539673e-05 0.9999865686 ± 2.02074847e-05	0.0318902 0.0255714 0.000232165 0.999985
		Protein Amounts (Arbitrary Unit – AU) unknown_kinase	assumed = IRS1_PI3K	2.965

Table S3. Parameter values of hypotheses 1, 2, and 3. For each hypothesis, the estimated parameters were calibrated using the same protocol provided in table S2. For each hypothesis, all the corresponding calibrations converged to a single solution set.

Model	General Model	TSC1/TSC2-dependent Hypothesis	NFL-dependent Hypothesis	PI3K-independent Hypothesis	4 th Hypothesis
Total χ^2	43.8073	45.9226	43.4833	43.33	43.33
Total Time Points (N)	99	99	99	99	99
Total Estimated Parameters (k)	30	30	30	32	32
AIC	434.2002	438.8688	433.4653	437.1157	437.1157

Table S4. Summary of model goodness of fit. The total chi-square and Akaike Information Criterion (AIC) measures are reported for the general model and the four hypotheses. Both the measures slightly penalize the TSC1/TSC2-dependent hypothesis. AIC also penalizes the PI3K-independent and the fourth hypotheses due to the higher number of parameters in these two models. However, these differences are not statistically significant for rejection of any model.

Model S1. General Model. The general model in Systems Biology Markup Language (SBML). Filename: general_model_sbml.xml; file size: 82.2 KB.

Model S2. Hypothesis 1. The model file for Hypothesis 1: TSC1/TSC2-dependent mTORC2 regulation. Filename: tsc1-tsc2_dependent_hypothesis_sbml.xml; file size: 82.3 KB .

Model S3. Hypothesis 2. The model file for Hypothesis 2: NFL-dependent regulation of mTORC2. Filename: negative_feedback_dependent_hypothesis_sbml.xml; file size: 82.3 KB .

Model S4. Hypothesis 3: PI3K-independent regulation of mTORC2. Filename: pi3k_independent_hypothesis_sbml.xml; file size: 86.4 KB .

Model S5. Hypothesis 4: PI3K-dependent, NFL-independent regulation of mTORC2. Filename: 4th_hypothesis_sbml.xml; file size: 85.7 KB.

Model S6. Full extended model. This corresponds to the Systems Biology Graphical Notation (SBGN) model shown in fig. S1. Filename: extended_mtor_model_sbml.xml; file size: 369.3 KB.